Artificial Intelligence Review
https://doi.org/10.1007/s10462-022-10231-3

An active deep learning method for diabetic retinopathy detection in segmented fundus images using artificial bee colony algorithm

Erdal Özbay[1]

Abstract
Retinal fundus image analysis (RFIA) is frequently used in diabetic retinopathy (DR) scans to determine the risk of blindness in diabetic patients. Ophthalmologists receive support from various RFIA programs to cope with the detection of visual impairments. In this article, active deep learning (ADL) using new multi-layer architecture for automatic recognition of DR stages is presented. In order to facilitate the detection of retinal lesions in the ADL system preprocessing, the image is segmented using the artificial bee colony (ABC) algorithm with a threshold value determined according to the results of the image histogram. Besides, a tag-efficient convolutional neural networks (CNN) architecture known as ADL-CNN has been developed to automatically extract segmented retinal features. This model has a two-stage process. In the first, images are selected to learn simple or complex retinal features using basic accuracy labels in the training examples. Second, useful masks are provided with key lesion features and segment areas of interest within the retinal image. Performance evaluation of the proposed ADL-CNN model is made by comparing the most advanced methods using the same dataset. The efficiency of the system is made by measuring statistical metrics such as classification accuracy (ACC), sensitivity (SE), specificity (SP), and F-measure. The ADL-CNN model applied to the EyePacs dataset containing 35,122 retinal images yielded 99.66% ACC, 93.76% SE, 96.71% SP, and 94.58% F-measure. In this respect, it can be said that the proposed method shows high performance in detecting DR lesions from various fundus images and determining the severity level.

Keywords Artificial bee colony · Active deep learning · Convolutional neural network · Diabetic retinopathy · Image segmentation

✉ Erdal Özbay
erdalozbay@firat.edu.tr

[1] Faculty of Engineering, Computer Engineering, Firat University, 23119 Elazig, Turkey

1 Introduction

Diabetes mellitus (DM) is a globally prevalent chronic disease that develops when the body cannot produce enough insulin or cannot use the insulin hormone it produces effectively and can cause serious complications (Blair 2016). Today, approximately four hundred and fifty million people suffer from DM (Cole et al. 2020). This disease has nearly doubled in prevalence in the last 20 years (Ting et al. 2016). According to data from the International Diabetes Federation (IDF), DM may rise by about 8% by 2030 (Washington et al. 2014). It is predicted that by 2040, the number of people with DM will reach approximately 600 million, and approximately 200 million of these will be diagnosed with diabetic retinopathy (DR), a chronic eye disease that results in vision loss (Congdon et al. 2003; Sinclair et al. 2020). DR is one of the complications of diabetes and is a retinal eye disease that can lead to blindness along with various visual disorders (Annapoorani et al. 2021).

There are two types of DM that type-1 diabetes and type-2 diabetes. Type-1 diabetes is often seen in childhood or adolescence as a result of environmental and immunological factors and a lack of insulin hormones (Ting et al. 2016). An average of 85% of these patients shows DR signs. Type-2 diabetes is the type that occurs when body cells do not respond to insulin, which is common in middle-aged people. An average of 60% of those who have had diabetes for more than 15 years show signs of DR (Abbas et al. 2017). The process of DR causing vision loss progresses very quickly. Since the disease does not show certain symptoms in this process, early diagnosis becomes difficult. In this respect, regular screening of DR signs in DM patients is important in terms of reducing the risk of blindness and controlling the progression of the disease. Thus, blindness can be prevented with early screening and regular drug therapy, which is appropriate for DR patients (Li et al. 2018).

Ophthalmologists often use digital fundus imaging tools to diagnose DR. Fundus imaging is an imaging method that allows to show the conditions of the optic nerve, macula, retina, blood vessel, points called lesions and the structures of the bottom of the eye such as vitreous in color (Cockburn 2013). Figure 1 illustrates the structure of the retina and various DR lesions in a fundoscopic image. Lesions can be distinguished from each other in terms of red and bright hues. Small dark red ones are called microaneurysms (MAs) and larger ones in the form of bleeding are called hemorrhage (HEM). Bright spots are divided into soft or hard exudates (EXs). The bright yellow dots are hard exudates, while the yellowish-white dots are soft exudates, also called cotton wool (CW) caused by nerve fiber damage (Bhaskaranand et al. 2016). Clinicians recommend that DR patients undergo fundus analysis every six months throughout their life and annual fundus analysis for non-patients. These regular clinical examinations create a huge workload for experts to cope with (Akilesh et al. 2017).

Determining the severity of DR, as well as diagnosing DR is a very important challenge for treatment. DR stages are basically grouped into two classes as proliferative DR (PDR) and non-proliferative DR (NPDR). However, there are three distinct stages of NPDR they not considered healthy and PDR, namely mild DR which is the earliest stage of DR, moderate DR, and severe DR depending on the level of retinal defect (Haneda et al. 2010). Figure 2 shows EyePacs dataset samples of five stages of different DR severity levels depending on the retinal disorder level. The characteristics of the DR stages formed according to the types and number of lesions on the retina in fundus imaging are given in Table 1. The most important difficulty of the DR detection problem is that the images of mild and sometimes moderate DR signs are similar to those of No-DR. In this respect, visual similarities in the

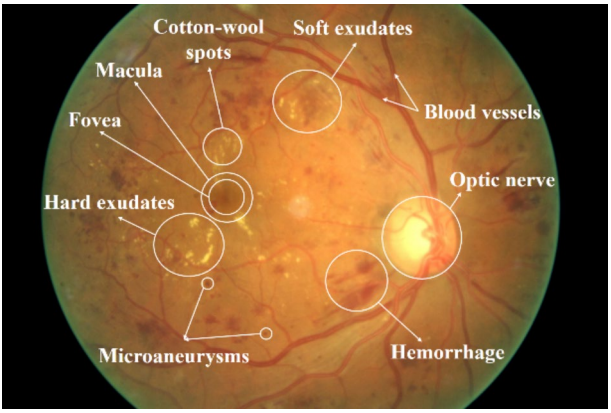

Fig. 1 A fundus sample with common lesions of DR

Fig. 2 EyePacs dataset samples for five stages of DR severity levels (0–4)

Table 1 DR stages depending on lesion characteristics

DR Levels	0-No-DR	1-Mild	2-Moderate	3-Severe	4-PDR
Lesions	No	only MA	more MA < severe DR.	20 < HEM venous beading	neo-vascu-lariza-tion pre-retinal HEM

early stages lead to uncertainties in the diagnosis process. If DR, which cannot be detected at these stages, progresses, it causes visual disturbances (Mateen et al. 2020).

Fundus images show varying degrees of symptom manifestation at different levels of DR severity. The earliest sign of DR is blood vessel lesions with small circular red dots. Moderate signs of DR are MAs, HEMs, EXs, and CWs. However, the ratio of these symptoms is important in determining mild and severe levels. The PDR level requires the formation of new blood vessels alongside these abnormalities. An important problem in determining the level of DR severity is the visual similarity of symptoms between No-DR, Mild-DR, and sometimes Moderate-DR, making it difficult to identify in the early diagnosis stages. For this reason, if DR progresses to an advanced stage, vision loss may occur in the person (Majumder et al. 2021).

Researchers have made fundus imaging available to CAD tools and ophthalmologists as a painless and non-invasive method for determining the level of DR (Lin et al. 2020). They

can make some evaluations by analyzing the distinctive features of DR lesions such as MAs, HEMs, EXs, and CWs of the retina (Li et al. 2019a, b). MA causes a variety of disorders caused by blood or fluids leaking into the retina, and its very few occurrences on fundoscopic images indicate the onset of DR (Pratt et al. 2016). When the No-DR lesion signs are examined, it is observed that there is no blood or fluid leakage in the retinal vessels. At least one MA sign is found in the mild DR stage, other than that there are no HEM, EX, or CW (Guo et al. 2019). In the moderate DR stage, many MA findings are observed, although less than in the severe DR stage (Li et al. 2013). However, in the severe DR stage, signs such as multiple MA, more than 20 HEMs in each of four quadrants, venous beading in two quadrants, or intraretinal vessel irregularity in one quadrant can be observed (Alyoubi et al. 2021). PDR is determined with various DR lesions, blood vessels, pre-retinal vitreous, and optic disc size assessment. Differences in retinal images obtained with fundus imaging and the complex nature of DR lesion components make it difficult for clinicians to diagnose DR (Kermany et al. 2018). In addition, the DR rating made by experts is subjective. Moreover, the inter/intra-reader must present his technical domain knowledge with precision. In this regard, computerized tools are needed to reduce the variability between clinicians of DR assessments and to perform them more clearly (Mansour 2018)

Various computer-based methods have been developed in many studies on the detection of DR. In these studies carried out, automatic detection of the characteristics of the lesions was emphasized in order to imitate the sensitive interpretations of the experts in the detection and grading of DR (Pires et al. 2013). Because manual diagnosis and grading of DR by ophthalmologists requires great effort and time. However, by using computer-aided systems to diagnose and grade DR, misdiagnoses can be prevented and overall cost, effort, and time can be reduced. Some of the studies implemented in image processing approaches via retinal images by using computer-aided systems have addressed the problems of detection and segmentation of blood vessels (Goatman et al. 2010), MA detection (Cao et al. 2018), EX detection (Wisaeng et al. 2019), neovascularization, and lesion detection (Kar et al. 2018).

In the studies in the literature, deep learning (DL) approach has emerged in the last decade, and its use has become popular in many fields, especially in medical and medical image analysis subjects in the last few years. Studies have shown that in segmentation and classification, the features of the input data can be defined more accurately and precisely, and higher performance can be achieved compared to traditional image analysis methods. A deep learning model (DLM) is a multi-layered machine learning (ML) method that can predict results by learning high-level abstractions with a given dataset. In this regard, while DL does not need hand-crafted feature extraction, it requires significant data for training (Deng et al. 2014). In studies of DR detection using ML techniques, the vessels must be extracted first (Vega et al. 2015). Subsequently, the focus is on extracting the features of DR lesions (Sikder et al. 2021). However, DL applications are a very effective image analysis tool that successfully carries out processes directly such as classification, segmentation, acquisition, detection, and retrieval (Bakator et al. 2018).

A deep convolutional neural network (CNN) is a highly effective and successful DL method that is frequently used in image analysis (Lu et al. 2017; Litjens et al. 2017). Thus, the success and effectiveness of DLMs have been proven by studies in the fields of biomedical image analysis and computer vision (Zhang 2018). Many CNN studies have been produced for the successful classification of natural medical images using fundus images with high sensitivity and specificity. More efficient and effective results have been obtained from

these studies, in terms of direct DR detection and grading compared to traditional feature extraction-based methods (Galveia et al. 2018).

Although many deep CNN architectures that undertake DR diagnosis and grading studies have achieved successful results, there are still various constraints and limitations. These are as described below.

- Current CNN models have focused only on an end-to-end DR grading without yet detecting the location of DR lesions in fundoscopic images. Here, the input images are fed directly into CNN, and the image outputs affect the severity level of the DR. Whereas, the clinical details of DR lesions are of great importance for ophthalmologists.
- In particular, a comprehensive CNN model needs an extensive and broadly annotated dataset. Significant time-consuming tasks and high costs are spent to obtain it and make it usable.
- Some developed CNN models have difficulties in learning the complex lesion structures caused by DR. Small patch of fundus images used as CNN inputs made it difficult to locate many small lesions such as MA and HEM due to their indistinct shapes. Therefore, it is vital to learn lesions with small details for DR detection and grading systems.

In order to overcome these problems, a multi-layered architecture developed with active deep learning (ADL) based on CNN models is proposed. The main contributions offered by the developed ADL-CNN system are as described below.

- A new ADL-based architecture is presented to efficiently recognize and grade detailed DR lesions with five different classes. This ADL-CNN model can learn and segment more accurate DR lesion features with fundus samples.
- ADL-CNN is executed with all the parameters of the CNN model to select the relevant patches and images in the DR assessment. It enables training samples to be recognized using a single backward-forward pass, which allows for variability in parameters for learning.
- The retina imaging preprocessing step is integrated into this work to highlight the enriched features in the DR severity level definition. The uncertain DR lesion features are clarified and stronger feature learning is provided with the image preprocessing performed using the artificial bee colony (ABC) algorithm.
- The efficiency of the proposed ADL-CNN architecture is demonstrated by making comparisons with state-of-the-art systems.

The next sections of the article are presented in the following order. Section 2 has the current literature on CNN-based DR detection works. Section 3 presents proposed methodologies along with materials and methods in detail. Section 4 is covered the experimental results. The discussion is presented in Sect. 5. Finally, the conclusion is mentioned in Sect. 6.

Table 2 Experimental results of classification studies using DL for DR detection

Category	Study	Lesion Detect	# of Class	ACC (%)	SE (%)	SP (%)
Binary	Liu et al. 2019	-	2	90.84	90.94	95.74
	Jiang et al. 2019	-	2	88.21	85.57	90.85
	Das et al. 2021	-	2	98.70	99.60	98.20
	Pires et al. 2019	-	2	-	-	-
Multi-level	Hsieh et al. 2021	-	3	-	-	-
	Khan et al. 2019	-	4	98.15	98.94	97.87
	Zhang et al. 2019a, b	-	4	96.50	98.10	98.90
	Shanthi et al. 2019	-	4	96.35	92.35	97.45
	Wang et al. 2018	-	5	63.23	-	-
	Wan et al. 2018	-	5	95.60	86.40	97.40
	Harangi et al. 2019	-	5	90.07	-	-
	Li et al. 2019a, b	-	5	65.10	-	-
	Dekhil et al. 2019	-	5	77.00	-	-
	He et al. 2020	-	5	85.69	-	-
	Kassani et al. 2019	-	5	83.09	88.24	87.00
	Bodapati et al. 2021	-	5	82.54	83.00	-
	Akilesh et al. 2017	-	5	89.00	90.00	88.00
	ResNet 2015	-	5	95.00	91.00	93.00
	SeNet 2018	-	5	87.00	82.00	90.00
	DenseNet 2017	-	5	89.00	88.00	89.00
Hybrid-(Lesion localized)	Orlando et al. 2018	Red lesion	2	83.68	54.47	93.65
	Zago et al. 2020	Red lesion	2	-	94.00	-
	Li et al. 2019a, b	All	5	92.95	99.39	99.93
	Wang et al. 2020	Red lesion	5	-	92.59	96.20
	Gulshan et al. 2016	All	5	-	97.05	93.39
ADL-CNN	**Our proposed**	**All**	**5**	**99.66**	**93.76**	**96.71**

2 Related works

In the past years, many handcraft feature-based classifications have been made to detect and grade the DR severity level from fundoscopic images (Mookiah et al. 2013). However, these methods focused only on the segmentation of candidate regions of DR lesions. DL is divided into three basic categories, which use CNN extensively in fundoscopic image classification and localization studies for DR detection and grading.

The first of these is the binary DR classification. These studies propose an end-to-end CNN to detect referable or non-referable DR images. Although respectable results have been obtained for DR detection in these studies, they did not include the DR severity level and the various lesions causing DR. In this respect, the most important disadvantage of studies using binary classification is that they are evaluated in only two categories, regardless of five different DR severity levels.

The second is multi-level classification studies that review DR detection according to different severity levels. Although the CNNs suggested in these studies produced successful results in DR detection and severity level classification, the inclusion of DR lesion localization in these studies is insufficient for ophthalmologists to make a diagnosis. As shown in Fig. 3 (a), approximately 73% of the available studies had classified fundoscopic images

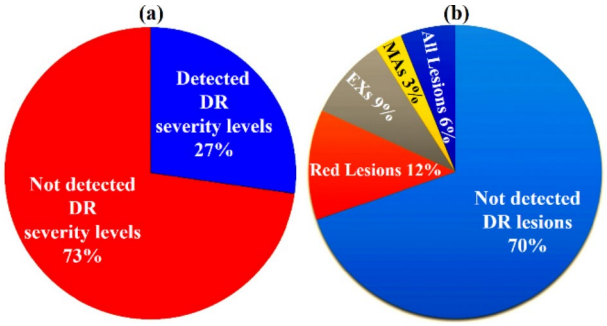

Fig. 3 The ratio of studies that detected DR severity levels (a) and classified DR lesions (b)

using DR or non-DR binary classifiers, while 27% classified the input with one or more stages (Alyoubi et al. 2020).

The third category is hybrid classification. This section covers studies that co-classify DR lesion localization as well as DR detection and grading from fundoscopic images. When the existing studies are examined, it is seen that the number of studies that localize the DR severity level and DR lesion types on fundus images are limited compared to all DR classification studies. Figure 3 (b) shows the ratio of all studies localized by lesion types in the present DR detection studies. While approximately 70% of the studies do not localize any DR lesion, only about 6% perform DR lesion localization over all fundus images. High-accuracy lesion localization of DR diagnosis and grading is a critical requirement for DR patient follow-up and treatment (Li et al. 2021). Table 2 comparatively summarizes recent efforts with DR classifications in these described three categories.

Successful performances have been demonstrated in previous studies using CNN in the diagnosis of DR. In one of these studies, a DR severity stage classification was performed on the Kaggle data science platform, which includes 8 thousand images. In this regard, they developed a CNN architecture with the data augmentation technique and classified five different severity levels of a DR that determined complex DR lesion features such as MAs, HEMs, and retinal EXs. 75% accuracy (ACC) and 95% sensitivity (SE) values have been achieved with the experimental results obtained from 5 thousand validation set (Pratt et al. 2016). In another study, 128 thousand fundoscopic images have classified by applying a CNN developed with the support of an ophthalmologist. This DR severity-level classification has obtained 97.5% SE and 93.9% SP with this proposed CNN model (Gulshan et al. 2016). In another study, a data-augmented CNN architecture is proposed for DR diagnosis. This proposed method achieved an accuracy rate of 93.28% (Raju et al. 2017). In a different method using the CNN model, DR was classified as normal, mild, moderate and severe DR with 94% accuracy (Sankar et al. 2016). The classification power of the CNN model at the five-class DR severity level is increased by the use of convolutional and maximum pooling layers together with the dropout layer (Chandrakumar et al. 2016). The proposed CNN method has achieved 96% success. In a different semi-supervised deep learning method that does not use any pre/post processing, the five-class severity level of DR has been determined. With this method, very successful classification results have been obtained (Abbas et al. 2017). A different method for DR detection, which classifies 35,126 images with the Alexnet-based CNN model, achieved an accuracy rate of 97.93%.

An ADL learning scheme has been developed to classify the sentiment of the document in one study (Zhou et al. 2014). In another study, an ADL method using fewer queries

has been proposed to measure the predictions of the Gaussian process regression model (Freytak et al. 2014). ADL has reduced the need for large expert-labeled samples for DR diagnosis. One study compared two ADL learning schemes involving query-by-bagging and uncertainty sampling (Sánchez et al. 2010). Here, selecting the most informative patches to be used for training multiple CNNs increases the computation cost.

Besides all classification studies using DL for DR detection with experimental results, there are also some valuable studies using some related multi-layer structures in the community such as IoT-Perceptive human activity recognition (Zhang et al. 2019a, b), multi-process collaborative architecture for time series classification (Xiao et al. 2021), and end-to-end multimodel deep learning for malware classification (Snow et al. 2020).

In this study, to address the shortcomings of the existing studies described in the previous section, high-feature images and patches are automatically selected for DR severity level grading, and a DL method generates viable masks for the estimation of relevant DR regions is proposed. For this reason, instead of a complete data set, an ADL schema was created with a training set with high learning characteristics. Thus, ADL can achieve higher accuracy by using fewer training samples. As a result, a realistic CAD system can be developed by avoiding the data labeling time and costs of experts with this method (Yu et al. 2015). This work uses an ADL scheme to train the 7-layer CNN architecture on fundoscopic images for DR lesion detection and classification of five different severity stages. In this regard, it is presumed that this is the first time combining an ADL schema with a preprocessing of images using the ABC optimization algorithm to identify features.

In the first step of the proposed method, the noise in the images is removed by using morphological filtering because the formation of fundus databases includes images with different resolutions and illumination types collected from different sources. Then, the ABC algorithm was used to find the optimum threshold value for the detection of different DR severity levels. Thus, a clear structure was created for the separation of levels. In the next step, one of the active learning methods a two-stage CNN architecture known as ADL-CNN has been used. The ADLCNN system first selects both the most informative patches and images using some key truth tags of the training samples to learn the characteristics of different retinal symptoms. Next, the DR provides useful masks for segment interests in fundus images to grade the five severity levels. However, existing studies adopt either directly label-efficient CNN architectures or classification approaches over manually segmented dataset images. Although these approaches produce accurate results, they are not effective enough in determining the severity levels of DR and delay the determination of early diagnosis stages.

3 Proposed methodology

This paper proposes an ADL-CNN with multilayer architecture for the diagnosis of DR and its severity levels using color fundoscopic images. While developing the ADL-CNN system, some preprocessing steps are applied on fundoscopic images. Because fundus images contain some shadows, specular reflections, irregular illumination, noise figures, and DR lesions with different hues, noise removal, and contrast enhancement operations are performed in the color space. After the preprocessing, the proposed ADL-CNN model is used

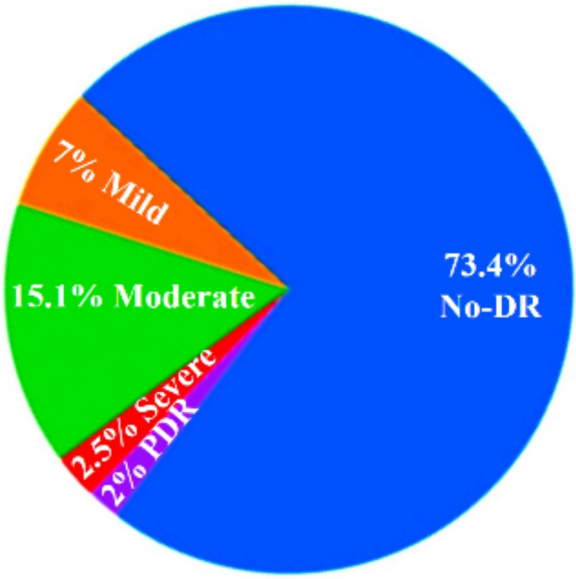

Fig. 4 The percentages of EyePacs fundus images per class

to detect the candidate region in the retinal image and to classify the different DR severity levels.

3.1 Dataset

The EyePacs dataset has been used in the training of the ADL-CNN model realized in the study. The retinal image database contains 35,122 images with varying degrees of DR supported by the California Health Care Foundation (Christine 2015). This diversity allows the recognition of different retinas in real-world environments. The EyePacs dataset contains a large collection of high-resolution retinal fundus images captured under different imaging devices and varied light conditions. Each subject includes two separate images, one for the left eye and one for the right eye. The dataset contains fundoscopic images with five different classes: 0-No-DR, 1-Mild, 2-Moderate, 3-Severe, and 4-PDR. The number of images belonging to the classes are 25,806, 2443, 5292, 873 and 708, respectively. Each sample is evaluated by ophthalmologists between 0 and 4 DR classes. In this regard, level 0 indicates healthy individuals, 1, 2, and 3 indicate mild, moderate, and severe DR respectively, while level 4 indicates PDR. The percentages of images of the classes to which the dataset belongs is given in Fig. 4.

3.2 Pre-processing

Detection of DR lesions from fundoscopic images is an important and challenging task. Images taken with digital imaging devices have various reflections and shadows due to masking on DR lesions. Effects such as some bubble appearances, tinted lesions, specular reflections, uneven lighting, and noise are part of the fundoscopic images. In this preprocessing section, it is aimed to facilitate DR lesion detection based on the ABC algorithm

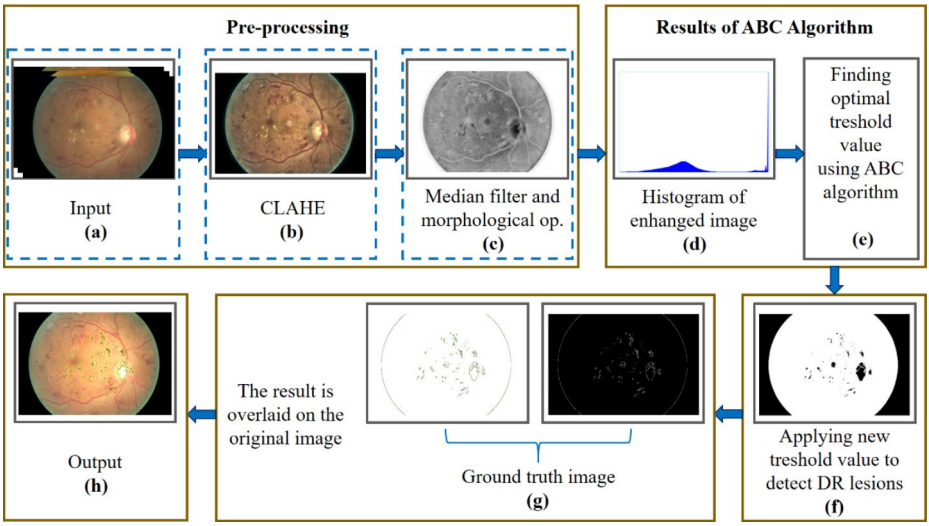

Fig. 5 DR lesions segmentation of fundoscopic images using ABC algorithm

method. The proposed methodology focuses on decontextualizing DR lesions without damaging their colour, geometry, and shape, that is, making them prominent in the image. The flowchart of the pre-processing methodology is shown in Fig. 5.

The fundoscopic images of the polymorphic database caused by the environment and constraints based on different devices, different resolutions obtained from different sources, lighting, etc., are passed through morphological filtering in a pre-processing step and the noise in the images is removed. In this context, the proposed method should remove unwanted spatial structures and reduce their ratio in fundoscopic images. However, it should highlight prominent lesion features without compromising any segmentation system. This challenge leads to the need to develop diverse and robust solutions for DR detection and segmentation of lesion markers in retinal images and disease severity grading (Porwal et al. 2020).

The illumination level can lead to the formation of unnecessary variations that are irrelevant as well as revealing some distinctive features. In the preprocessing step a contrast-limited adaptive histogram equalization (CLAHE) filtering algorithm has been implemented to increase classifier sensitivity via OpenCV to highlight some obscure features of DR lesions in the dataset and to remove some irrelevant features. The CLAHE method is a filtering and histogram equalization method developed for medical image enhancement systems, trying to reduce the noise produced in homogeneous areas (Singh et al. 2019). The result of CLAHE process is shown in Fig. 5 (b). It has been seen with the obtained accuracy results that this digital image preprocessing technique used provides better detection of sensitive point features through convolutional filters that could not be detected by CNN before. Then, morphological filtering based on Median and Gaussian kernels has been used to smooth out noises in fundoscopic images. Morphological filtering aims to improve the color of DR lesions to highlight their geometry without deforming them. Median filtering and a nonlinear function are implemented to the images converted to gray level, thereby removing the salt and pepper noise in the images. This pre-processing process is an effective process

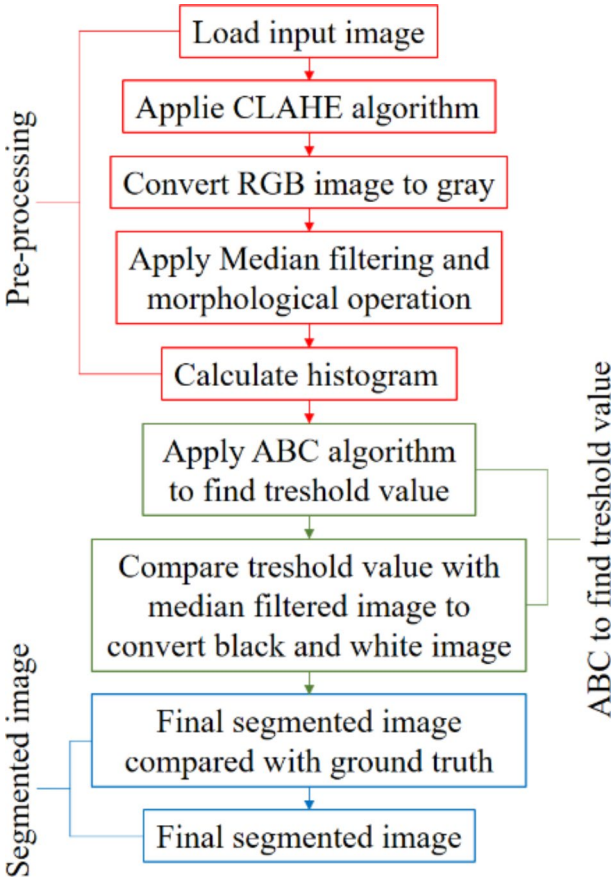

Fig. 6 The flowchart of DR lesions segmentation

for reducing the noise of the images and preserving the lesion edges. In this respect, it has very high importance before moving on to the convolution operations. 2D median and morphological filtering of 20×20 size have been implemented to smooth the noises. The steps implemented in this process are embedded in the image preprocessing system. The results of this process are shown in Fig. 5 (c). In the next step, the ABC algorithm is implemented to find the optimal thresholding value based on the histogram of the enhanced image as seen in Fig. 5 (d,e). We can find boundaries and segments of DR lesions by the optimal threshold value using the ABC algorithm, as seen in Fig. 5 (f). In order to evaluate the performance of the image pre-processing, the segmented image is compared with the ground truth image and the result obtained is overlain on the original fundoscopic image (Vaishnavi et al. 2016). Thus, the DR lesions have segmented and the enhanced image is shown in Fig. 5 (g). The flowchart for ABC-based DR lesions segmentation is given in Fig. 6.

Finally, the image is cropped in the middle and black corners are removed to focus on the fundus in the images. Fundoscopic data containing different stages of DR is resized to a 48×48 pixel patch. In the ADL-CNN model, randomly selected patches of each class consist of 15,520/2,628 patches as training/test.

3.3 Artificial Bee colony (ABC) algorithm

The artificial bee colony algorithm is a swarm-based optimization method inspired by the intelligent foraging of honey bees (Karaboga 2010). Its swarm-based nature is due to the fact that a group of honey bees fulfills their duties through social teamwork (Tsai et al. 2009). Bees are grouped into three classes in the ABC algorithm; worker, scout, and onlooker. Worker bees search for food near the food sources in their memory and transmit the location and quality information of the food to the onlooker bees through communication. Scout bee is decoded from a small number of worker bees that dispose of their food source. The swarm is divided into two separate branches in the ABC algorithm. Half of this group consists of workers and the remaining half of onlooker bees. A random initial population of food sources is generated by ABC with SR solutions of worker bees. SR represents the group number of bees.

$W_i = \left[W_{i,1}, W_{i,2}, \ldots, W_{i,N}\right]$ is assumed to be the *i*th solution of a group of bees and the length size is expressed with *N*. Each worker bee W_i wants to create a new contestant resolution C_i close to its location. This situation is expressed by Eq. (1).

$$C_{i,j} = w_{i,j} + \sigma_{i,j}.(w_{i,j} - w_{k,j}) \tag{1}$$

where *w* is the arbitrary contestant resolution (*i* cannot be equal to *k*). *j* is a randomly selected length index from the group. $\sigma_{i,j}$ is a randomly determined number in the range of -1 to 1. A hungry selection is preferred when a new candidate resolution C_i is desired to be created. If the fitness value of C_i is higher than the value of previous W_i, W_i is revised using C_i, otherwise, maintained w_i is fixed as constant. After the search processes of all worker bees are completed, information about food sources is transferred through the vibration movements of onlooker bees with each other. In the light of this information, the onlooker bee calculates the amount of nectar and selects different edible sources in addition to these related probabilities (Otsu 1979). Probability selection (P_i) acting as a roulette wheel selection (RWS) method is given in Eq. (2).

$$P_i = F_i / \sum_{j=1}^{SR} F_i \tag{2}$$

where F_i represents the amount of fitness at the *i*th resolution in the observed group. *i* is a superior resolution and a higher probability priority choice for *i*th nutrient sources. When the location cannot be further developed with a limited number of iterations, the food source is discarded. Assuming the discarded source is W_i, the scout bee uses Eq. (3) to determine a new food source, W_i.

$$w_{i,j} = LB_{i,j} + r(UB_{i,j} - LB_{i,j}) \tag{3}$$

here *r* is a random number based on a normal distribution between 0 and 1. *LB* is the lower and *UB* is the upper limit, with the corresponding *j*th length size. ABC algorithm steps are detailed in Algorithm-1.

Some metaheuristic optimization algorithms can be run to support the detection of DR lesions (Sreelatha et al. 2021). One of these suggested approaches for improvement is the

ABC algorithm (Vaishnabi et al. 2016). Studies on this subject have proven that the ABC algorithm can achieve higher results compared to other existing optimization algorithms (Khomri et al. 2018).

Algorithm-1 Artificial bee colony (ABC) algorithm.

1: Arbitrarily initialize the group of bees.
2: Update the solution for the initial swarm.
3: for every worker bee, a new candidate resolution C_i is produced based on Eq. (1). Calculate the
fitness of C_i and a hunger selection is utilized to select a superior one between W_i and C_i as the new W_i.
4: Each onlooker bee evaluates P_i with Eq. (2).
5: Produce a new candidate resolution C_i with Eq. (1) and the present solution (food resource).
Calculate the fitness of C_i and a hunger selection is utilized to select a best one between W_i and C_i like the
new W_i.
6: The scout bee finds the discarded W_i, if it stays and updates it with Eq. (3).
7: Update the superlative resolution institute until now, so iteration = iteration + 1.
8: if the amount of iteration exceeds maximum number of iteration, then
9: after that stop the process and display the output results;
10: else
11: Repeat Step 2.
12: end

3.4 Architecture of ADL-CNN model

CNN is an important deep learning framework inspired by the hierarchical working logic of the human visual cortex. The developed model identifies graphic patterns by learning abstractions with training data. In order for the training of the CNN model to obtain accurate predictions, objects are not allowed to change their position invariance or become distorted. In particular, additional inputs are used as a data augmentation advantage in improving the localization capabilities of CNN models in medical imaging applications (Greenspan et al. 2016; Otálora et al. 2017).

Our ADL-CNN model is inspired by the LeNet model structure, which consists of a patch input layer followed by two convolution and two max-pooling layers and a fully connected layer (Zhang 2018). Softmax, the last layer of the 7-layer model, is a classifier that evaluates the probability of patches being normal or abnormal. In line with the obtained experimental results, it was seen that the system using the forward-backward transition produced high classification results by choosing highly informative images despite fewer inputs. The architecture of the proposed ADL-CNN model developed for DR detection and severity grade is illustrated in Fig. 7.

The proposed model uses RGB channels in each pixel in the image patch (X_i, Y_i) of 48×48×3 fundoscopic input images. Twenty 5×5×3 kernels are used for the convolution-1 layer operation to be applied to the input size. Next, the max pooling-1 layer of size 2×2 is

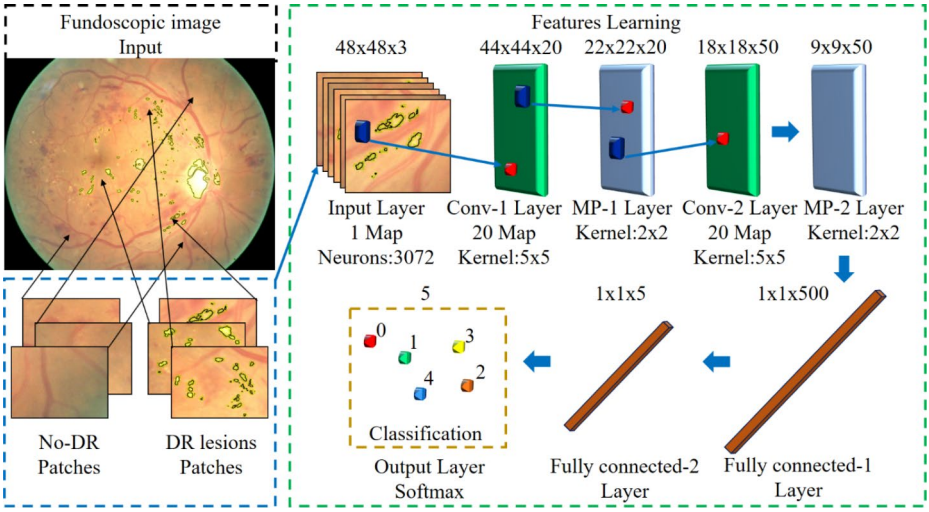

Fig. 7 Proposed ADL- CNN architecture to classify DR severity-level

Table 3 The parameter structures of the used CNN model

Layers/Type	#of feature maps	Output shape	Kernel size - for feature map	Trainable parameters
0 / Input	3	48×48×3	-	-
1 / Convolution	20	44×44×20	5×5×3	448
2 / Max-pooling	20	22×22×20	2×2	-
3 / Convolution-2	50	18×18×50	5×5×20	4640
4 / Max-pooling-2	50	9×9×50	2×2	18,496
5 / Fully-connected	-	1×1×500	-	32,896
6 / Fully-connected-2	-	1×1×5	-	516
7 / Soft-max	-	5	-	56,996

processed. A reapplied convolution-2 layer is executed between fifty 5×5×20 kernels and twenty feature maps. Next, the max pooling-2 layer of size 2×2 is processed again. Then all the neurons of layer 4 are fully connected to the 500 neurons of layer 5. Then all the neurons of layer 4 are transferred to 500 neurons in the fully connected-1 layer. Similarly, all neurons in layer 5 are transferred to 5 neurons in the fully connected-2 layer. The last layer of the 7-layer architecture, the Softmax classifier layer, generates five classes of neurons in response to the inputs from layer 6 which shows 0-No-DR, 1-Mild, 2-Moderate, 3-Severe, and 4-PDR, respectively. In this regard, layer 7 successfully fulfills the task of classifying the neuron class with the highest probability. The parameters of the proposed ADL-CNN model is given in Table 3.

Various hyperparameters such as activation functions, learning and learning decay ratio, model depth, weight decay ratio, batch size, and momentum have been used in fine-tune and optimizing the training process of the ADL-CNN model. The values of the applied initial hyperparameters have been determined as learning decay ratio: 0.1, weight decay: $1x10^{-4}$,

and learning rate: $1\text{x}10^{-3}$. The rectified linear unit (ReLU) is used as the unit that performs the activation process in layers 1, 3, 5, and 6 with the activation function. The Gaussian distribution method is used in the Softmax layer to generate random biases.These weights and biases used in these layers are also included in other studies with proven suggestions (He et al. 2016).

AL aims to identify the best possible classification ways by annotating large amounts of unlabeled images of the image pool to enable deep learning algorithms to achieve higher accuracy results. ADL is a deep AL art where learning is used iteratively by completing each iteration together with the batch setting (BS). The method allows the generation of image classes designated by C along with the label $Y = \{1,\ldots, C\}$ and the compact space S of the image. The hypothesis class of DL art defined as S x $Y \rightarrow R$ is parameterized by w in a loss function accepted as $l(\cdot;\cdot;w)$. Since the regression functions are specific to each class, £$c=p$ $(y=c \mid x)$ ƛ£-Lipchitz for all c's is assumed to be continuous. Samples of data collection (*i.i.d*) is characterized as $\{x_i, y_i\}_{i\in[n]}\tilde{p}_z$ on the defined space $Z=S$ x Y, where $[n] = \{1,\ldots, n\}$. The initial pool of images selected as so = $\left\{s^0(j) \in [n]\right\}_{j\in[m]}$is handled consistently. The ADL examines the labeled samples that belong to the initial subsample pool as $\{x_i\}_{i\in[n]}$ and $\left\{y_{s(j)}\right\}_{j\in[m]}$. The system includes a b budget for queries and a learning art called As. This creates a set of parameters w to be obtained according to the outputs using a labeled set of s. AL solves this problem with Eq. 4 given below;

$$\min_{s^1:\left|s^1\right|\leq a} L_{x,y\tilde{p}_z}\left[l\left(x, y; F_{s^0\bigcup s^1}\right)\right] \tag{4}$$

Fewer losses than expected can be achieved by AL using budget b to select the extra samples that are labeled. The state of being equal to 1 of the budget b is taken into account in the known approaches. However, the budget b value alone has little effect on the learning level. In this regard, a dynamic budget set is adopted. The AL approach also considers various shots to be evaluated in multiple rounds to select informative samples in the analysis of a single sample labeling series.

$$\min_{s^{q+1}:\left|s^{q+1}\right|\leq a} L_{x,y\tilde{p}_z}\left[l\left(x, y; F_{s^0\bigcup \ldots s^{q+1}}\right)\right] \tag{5}$$

According to Eq. 5, the AL method handles image labeling in its first iteration when $q=0$, followed by an annotation tour for more images. The ADL algorithm has two stages; consulting an expert to explain the structure of the datasets and learning with the classifiers developed using previously explained samples. Creating image labels one by one by asking a clinician in the standard AL process means expressing the budget as $b=1$. Such applications are not at all advantageous for CNN, since local optimization algorithms have a negligible statistical effect. In addition, due to the abundance of artificial intelligence problems, it is difficult to train the CNN model with a set of image tags. Therefore, expert labeling of images at each iteration contributes to the batch setting of the AL algorithm. The upper limit of active learning loss is used as in Eq. 4 for this batch case. In the proposed algorithm, a small annotated subset s of the AL method is used to learn the population risk of the CNN network. Equation 6 is used after checking the population risk of the proposed model on a small number of labeled subsets;

$$L_{x,y\tilde{p}_z}\left[l(\,x,y;F_s\,)\right] \leq \|\, L_{x,y\tilde{p}_z}\left[l\left(x,y;F_s\right)\right] - \frac{1}{n}\sum_{i\in[n]} l\left(x_i,y_i;F_s\right)\|\ldots$$

$$+\frac{1}{|s|}\sum_{j\in[s]} l\left(x_j,y_j;F_s\right) + \|\,\frac{1}{n}\sum_{i\in[n]} l\left(x_i,y_i;F_s\right) - \frac{1}{|s|}\sum_{j\in[s]} l\left(x_j,y_j;F_s\right)\| \tag{6}$$

The difference between the empirical losses of the whole dataset and the unlabeled images reveals the core set loss. In this respect, core set loss and generalization error are provided over all data [n]. When the AL problem is structured considering the core set loss, it is defined as follow Eq. 7;

$$\min_{s^1:|s^1|\leq a} \|\,\frac{1}{n}\sum_{i\in[n]} l\left(x_i,y_i;F_{s^0\bigcup s^1}\right) - \frac{1}{|s^0+s^1|}\sum_{j\in s^0\bigcup s^1} l\left(x_j,y_j;F_{s^0\bigcup s^1}\right)\| \tag{7}$$

The initial annotated sample set $_{S^0}$ and budget b must be given together so that a collection can be selected in the query process of labels $_{S^1}$. Therefore, when the model completes the learning process, the entire dataset will perform closely with the network in the labeled sample set. While standard learning approaches use randomly labeled data in the model building process, the ADL approach is helpful in deciding which examples to label and which ones to include in training. This method starts with the evaluation of a labeled dataset at the beginning and continues with the learning of the more pertinent example and ends with the convergence of the annotated instances. The main goal of this approach is to obtain higher accuracy using a much smaller number of training samples by selecting data via the art of learning without having to use the entire dataset (Lin et al. 2016).

Stochastic Gradient Descent (SGD) is an optimization algorithm that can optimize a single specific sample batch group instead of the entire data set by calculating an objective function J over the defined model parameters θ (Otálora et al. 2017).

$$\theta_{t+1} = \theta_t - \eta\nabla J_i\left(\theta_t\right) \tag{8}$$

where $J_i\left(\theta_t\right)$is an objective function and evaluates the ith sample (x^i, y^i) at iteration t. η is the learning rate and ∇ refers to the gradient operator. When calculating the cost function $\nabla J_i\left(\theta\right)$ and its norm called gradient length term $\|\,\nabla J_i\left(\theta\right)\|$, the representative of the ith sample and its corresponding label must be determined. The important thing here is to determine how much of the contribution of the gradient length term with the sample and its label is required for each part of the gradient vector. Based on the analysis of the experimental results, we determined the learning rate η in Eq. 8 to be 0.01.

During the selection of the most informative patches in each batch iteration of the SGD, the samples with the highest values of the gradient length weighted according to the probability of finding the y^i label are performed. In other words, it is the selection of the instances whose labels are known to cause the greatest changes for the model being run.

$$\Phi(x^i) = \sum_{j=1}^{l} p\left(y^i = J\middle|\, x^i\right)|\,|\nabla J_i(\,\theta\,)|\,| \tag{9}$$

where *l* represents the total number of classes or labels. Φ refers to values sorted within an unlabeled sample pool and is used by the expected gradient length (EGL) algorithm to add as labeled to the training dataset. In the first of the studies that previously mentioned the concept of EGL, multi-instance active learning has been proposed (Settles et al. 2007). An expert is appointed to evaluate the ground-truth labels of the samples used in these studies and these are included in the training dataset. The specified method has been used to select the images of the CNN model in this study. Two terms of Eq. 9 have been calculated to select the most informative samples to be used in the CNN network. The first is the inclusion for calculating the probabilities of *j*th labels and the second is the corresponding probabilities of the Softmax layer. This CNN architecture is capable of backward/forward computation at certain layers. Since the deviations between the layers did not differ according to the experimental experience, the backward-stage has been applied after the first fully connected layers. This process is repeated on all possible labels of each sample with ground truth notions. After calculating the Φ value over all the samples in the data set, $k=64$ samples are selected for the highest EGL values ordered by sorting.

Algorithm-2. ADL patch selection in proposed CNN architecture.

Input: Labeled dataset (patch) $\mathcal{L}$,
Initial trained model *M* with patches in $\mathcal{L}? \subset \mathcal{L}$,
The most informative patches (number of *k* sample)
1: while no convergence do
2: create and shuffle sample batches from $\mathcal{L}$
3: for each batch do
4: Compute $\Phi(x)$ using *M*, for $\forall_x \in$ batch
5: end for
6: sorting all the Φ values and return the highest *k* samples $\mathcal{L}_k$
7: update *M* via $\mathcal{L}? \cup \mathcal{L}_k$
8: end while
Output: Patch *P*

As given in the algorithm in Algorithm-2, the first training of the *M* model with a part of the labeled dataset starts with $\mathcal{L}? \subset \mathcal{L}$ and continues by adding *k* samples to the $\mathcal{L}?$ parameter. This step, which is carried out to modify the M parameters, stops when the amount of training and testing error reducing or the accuracy remains constant for several epoch. Since this approach was successful in selecting the most informative patches, this approach was also adopted for the selection of the most informative images. In this respect, instead of estimating the EGL value of all images of the data set, densely computing the Φ value by patching high-feature images has facilitated the process. Then the images are sorted starting from the highest EGL value. Then, patches of the most outlier image are included in the training set during the parameter update process until convergence with Algorithm-2.

Algorithm-3. Image selection with ADL in a CNN.

Input: Labeled dataset (patch) $\mathcal{L}$, training set *T*, number *n* (initial images)
Randomly selecting intial set T_n of images
Initial training of model *M* from *n* images
1: while no convergence do
2: for each image in T / T_n do

3: Patchify image and compute $\sigma_{image} \sum_{patch \in \text{image}} \Phi(patch)$ using M
4: end for
5: Sort all the σ_{image}, return I_{max} (the image with higher sum)
6: $T_n = T_n \bigcup I_{max}$
7: $\mathcal{L}_n = \{patch \in \mathcal{L}_I, \text{for all} I \in T_n\}$
8: Update M with patches a $\mathcal{L}_n$ and k selected patches (Algorithm-2)
9: end while
Output: Image I

However, since it is not possible to manually label the images of the data set under the control of an ophthalmologist in this process, it is of great importance to training a label-efficient scenario with higher specification features. This process is explained by the algorithm given in Algorithm-3. This approach has preferred to select images that contain a few key features rather than train the entire dataset with the proposed model having an ophthalmologist label these images.

4 Experimental results

The performance evaluation of the proposed ADL-CNN model has been made on the EyePacs dataset containing dermatoscopic images. In this regard, it is shown that the ADL-CNN method is evaluated with measurable performance results for segmenting DR candidate region or lesions segmentation by selecting the most informative fundus images for classifying five different severity levels of DR.

This study combines the extraction of specific lesion information from images using the ABC optimization method with the development of the ADL-CNN system (Decenciere et al. 2013). The weight optimization of the ADL-CNN network using the Nesterov mode with the SGD optimizer application has been determined as a momentum value of 0.9. All training patches have been tested on a batch size of 32–64. In this regard, as a result of the experience gained, 32 batch sizes have been carried out in 30 epochs in which the learning rate has been used at 0.01 for the grid search. The proposed *M* model has been initially trained using 32 data samples from 5 batches.

Before DL, the image pre-processing process in which the data containing raw fundoscopic images were cropped, normalized and various filtering processes took a total of 12.8 s. Afterward, segmentation of DR lesions of fundoscopic images performed using the ABC algorithm took 14.7 s in Matlab R2021b environment. Standard data improvement and well-enhanced preparation before DL took a total of 27.5 s. Python 3.9 and Caffe DL tool were used to perform ADL-CNN system experiments (Cengil et al. 2017). The main reason for choosing these tools is to access parameters and data in memory efficiently. In the experiments, a machine with 16 GB RAM and Nvidia GeForce GTX 1080 graphics card was used. ADL-CNN system optimization of deep learning-based features took an average of 12.5 s to train, and an average of 1.6 s to create the final output layer. However, when the data was trained and tested, it was seen that approximately 7.8 s was spent for only classifying the images. This computation time for implementing ADL-CNN is 1.8 s longer

Table 4 Statistical performance metrics of the ADL-CNN system

		Predicted Class	
		Positive	**Negative**
Actual Class	**Positive**	True Positive (***TP***)	False Negative (***FN***)
	Negative	False Positive (***FP***)	True Negative (***TN***)

compared to current CNN models (Akilesh et al. 2017; Bello-Cerezo et al. 2019; He et al. 2015; Hu et al. 2018; Huang et al. 2017; Orlando et al. 2018; Perdomo et al. 2016). This difference is due to the use of new image pre-processing, DR lesion segmentation, and fast training techniques.

The training losses in the validation set were measured by the validation and accuracy tests. Statistical criteria such as ACC, SE, SP, and F-measure were used to measure the success of the proposed ADL-CNN model in determining the severity level of DR. Sensitivity (True Positive Rate, TPR) and specificity (True Negative Rate, TNR) are performance evaluation measures that measure the classifier's ability to accurately detect patient status as positive and negative, respectively. True-positive (TP) denotes positive values of the true state and classifier estimate, while false-positive (FP) denotes negative values of the true state. True-negative (TN) represents the negative values of both true and classifier predicted labels. True-negative (TN) shows negative values of both the true and the classifier estimate. False-negative (FN) indicates negative values of the classifier while the true class value is positive. Table 4 shows statistical performance metrics for calculation of ACC, SE, SP, FPR, and F-measure.

$$(ACC) = \frac{TP + TN}{TP + TN + FP + FN} \tag{10}$$

$$(SE) = TPR = \frac{TP}{TP + FN} \tag{11}$$

$$(SP) = \frac{TN}{TN + FP} \tag{12}$$

$$FPR = \frac{FP}{TN + FP} \tag{13}$$

$$F - measure = \frac{2TP}{(2TP + FP + FN)} \tag{14}$$

These experimental results demonstrate the effects of selecting patches of fundoscopic images containing the most informative features in the proposed ADL-CNN model, with Algorithm-3 rather than ophthalmologists. Figure 8 shows the training results of the ADL-CNN model. Accordingly, the red lines emphasize that the initial training was completed as shown in the graphs. Then, the most useful image patches are selected and the network parameters are updated using Algorithm-3. Here, patches of 4 training samples in the first 6 SGD iterations were preferred in executing the model training. At this stage, model con-

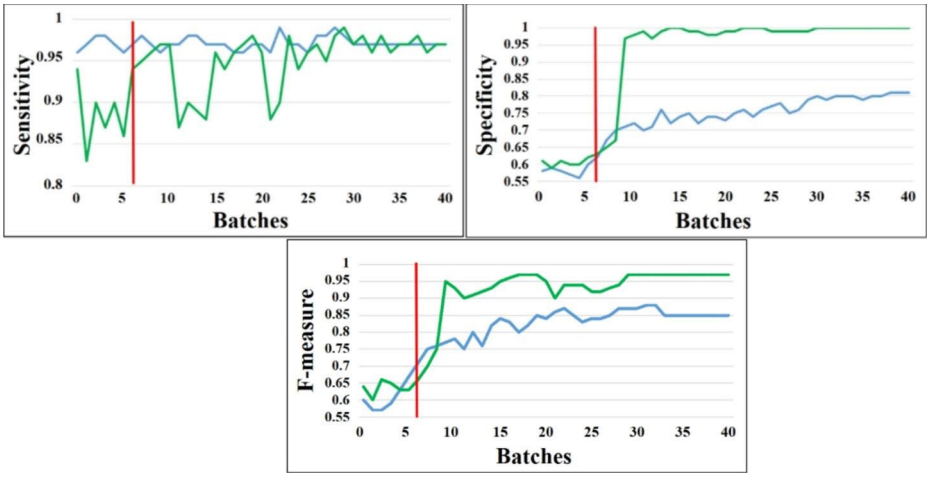

Fig. 8 Initial training results of the ADL-CNN model over SE, SP, and F-Measure (blue line) and AL (green line) for Algorithm-3. Red line indicates patches with the highest EGL value added to the dataset

vergence was achieved as early as 15 batches. Thus, it can be said that the proposed training procedure is superior to standard CNN models.

After the initial model training is completed, the most interesting full image is obtained as a result of the ranking by the sum of the EGL values. The output criteria for image selection are defined in Algorithm-3. Figure 8 shows a graphical representation of the interestingness values obtained at distinct training batch intervals. Figure 9 analyzes the change in the determination of interestingness value in the training intervals during further batch research. Here, we can understand that the interestingness value is decreasing, since the loss function no longer decreases or the model converges. In this case, the parameter norm is closest to 0 and indicates that the loss function will not decrease anymore.

35,122 digital retinal samples were used to evaluate the performance of the proposed ADL-CNN method. The values obtained for four different performance evaluation criteria, namely ACC, SE, SP, and F-measure criterion were compared for DR diagnosis. The results obtained with the proposed ADL-CNN method are listed in Table 5. When the values in this table are examined, it is seen that 99.66% for ACC, 93.76% for SE criterion, 96.71% for SP, and 94.58% for F-measure. These values show that an improvement has been achieved compared to the existing methods. The best values obtained for the No-DR class were 99.78%, 95.75%, 99.36%, and 99.98% for the ACC, SE, SP, and F-measures respectively, while the best values obtained for the mild diabetes class were 95.59%, 94.02%, 98.62%, 96.61%, respectively for the same criteria. Superior results recorded for moderate diabetes class with 94.58%, 90.05%, 94.88%, and 93.56%, respectively, for severe diabetes class 91.53%, 89.95%, 93.75%, and 92.54, respectively, and proliferative DR 90.51%, 90.97%, 93.87%, and 91.53%, respectively. The training error was created for each class as shown in Table 5. In this respect, the average training error value was obtained as 0.528.

We compared these experimental results with the current state-of-the-art classification methods that transfer learning (TL) (Gulshan et al. 2016; He et al. 2015; Huang et al. 2017) and DL studies (Akilesh et al. 2017; Orlando et al. 2018; Wang et al. 2017). We have used the EyePacs dataset samples for testing which also were used in their benchmarking studies.

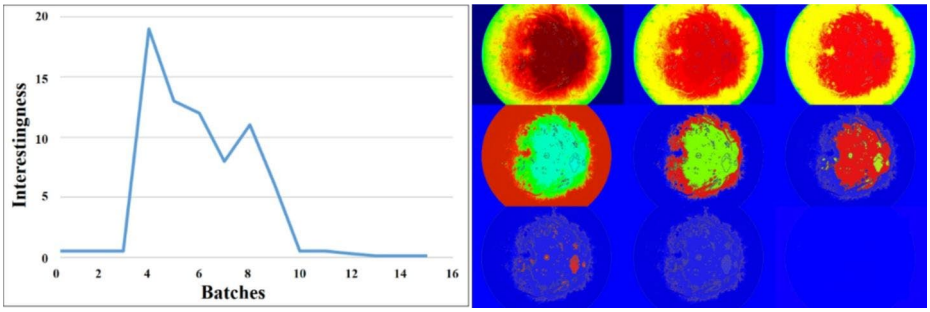

Fig. 9 Example of interestingness change over training time

Table 5 Performance evaluation of our ADL-CNN model for classification of five severity levels of DR on 35,122 segmented test samples

Severity level	Class	ACC (%)	SE (%)	SP (%)	F-measure (%)	Error
No-DR	0	99.78	95.75	99.36	99.98	0.436
Mild	1	95.59	94.02	98.62	96.61	0.445
Moderate	2	94.58	90.05	94.88	93.56	0.540
Severe	3	91.53	89.95	93.75	92.54	0.663
PDR	4	90.51	90.97	93.87	91.53	0.501
Total results		99.66	93.76	96.71	94.58	0.528

Forward comparative results are given in Table 2. As a result, when our ADL-CNN system was compared with the existing DR severity level classification studies, it was seen that higher results were achieved especially in terms of ACC, SE, and SP values. However, the SE value obtained by our network is slightly lower than in these leading studies (Li et al. 2019a, b; Gulshan et al. 2016). It can be said that our proposed model is more stable compared to the pioneering studies that produced high results looking at the evaluation results summarized in Table 2. In general, it can be said with certainty that our proposed model outperforms these approaches (Akilesh et al. 2017; Gulshan et al. 2016; He et al. 2015; Huang et al. 2017; Orlando et al. 2018; Wang et al. 2017). The superiority of the proposed approach over these comparative arts in DR severity classification is due to two main reasons; the first factor is the application of the optimization-based image processing technique used for the preparation of raw input fundoscopic images. The proposed network was segmented and localized region-of-interest (ROI) with this approach, in order to learn very small DR lesions and retinal features more easily to support the DR severity level grading. The model has carried out with the help of this process was obtained higher accuracy and less loss for DR severity level classification. The second factor is the ADL approach, in which the most informative patch samples are chosen to be used during model training rather than full samples of the entire dataset. The main advantage of this approach is to reduce the computational cost by using fewer samples with discriminative DR lesion features during training. In this regard, this approach presented an ADL method used to train the network model more effectively and faster.

In another experiment performed to evaluate the performance of this study, the classification of the pre-train CNN models and the ADL-CNN model were compared. In this regard, classification configuration tests on different CNN architectures were evaluated. Python 3.9

Table 6 Configuration parameter settings used for Pre-train mode in VGG16 architecture

Models	Layers	Learning rate	Fixed momentum
VGG16	16	0.0001	0.9
Inceptionv3	48	0.0001	0.9
VGG16noFC1	15	0.0001	0.9
VGG16noFC2	15	0.0001	0.9

Table 7 Comparisons of ADL-CNN with CNN structures on 35,122 samples for DR severity levels

Models	ACC (%)	SE (%)	SP (%)
VGG16	82.83	79.84	81.83
Inceptionv3	83.68	84.23	86.42
VGG16-FC1	84.83	87.82	78.84
VGG16-FC2	90.81	77.84	89.82
Proposed ADL-CNN	**95.03**	**93.21**	**94.32**

and Keras deep learning library with Tensorflow backend are used in these executed CNN architectures. The details of the network hyperparameters are given in Table 6.

The CNN models given in Table 6 were inspired by the Alex-net model for VGG16 and its versions, and the ResNet model for Inceptionv3 (Krizhevsky et al. 2017; Sundar et al. 2018). All these models have a set of convolutional layers, maximum pooling, and fully-connected layers. Previous applications on these models were trained with the ImageNet database (Deng et al. 2009). These models can produce higher performance than other state-of-art CNN models since various filters can be readjusted using TL. FC1 and FC2 versions of the VGG16 model produced more effective results during training by using one fully connected layer instead of two fully connected layers. It demonstrated a stable experimental result with a dropout value of 0.65 for each fully connected layer.

The performance evaluation of our ADL-CNN system in comparison with other CNN models is given statistically in Table 7. Considering the experimental results obtained, it was seen that the proposed ADL-CNN model was superior to the pre-training CNN networks for DR severity level classification. The highest values among all results given in Table 7 are in bold. Based on these results, it can be said that the proposed approach gives better results compared to Inceptionv3, VGG16, and its two versions. VGG16-FC2 achieved the highest result among pre-training CNN models except for the ADL-CNN model, with 90.81% ACC and 89.82% SP values. However, this model achieved the lowest SE value among all CNN models with a value of 77.84%. In general, our ADL-CNN system introduces a pixel-based model approach that achieves higher performance values compared to its competitors and produces very realistic segmentation results for DR lesions. The ground truth and the results closest to it are shown in Fig. 10. These results were reflected by converting them into white-black forms so that DR lesions defined in different colors can be seen more clearly.

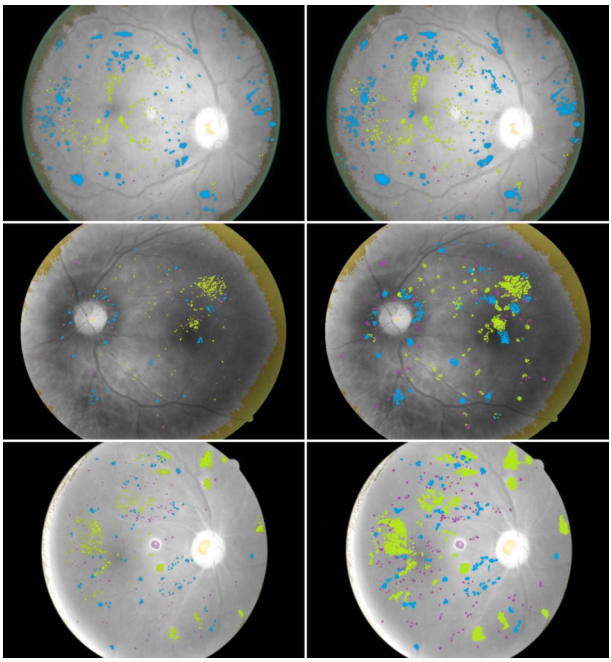

Fig. 10 Outputs for segmentation of DR lesions. Ground truth (left-side) and ADL-CNN results (right-side). Light green indicates EXs, light blue HEMs, and purple markings MAs

5 Discussions

This article establishes a reliable solution point for DR, a disease related to the human eyes. ABC optimization algorithm-based image quality improvement and DR lesion segmentation were applied to learn better DR features of fundoscopic images. Then, technologies based on patch-based image processing and multi-layer deep learning architecture were used to classify the severity level of DR. In the proposed technology, higher performance is achieved by using only the most informative portion of the selected images instead of training the ADL-CNN model over the entire data set (Perdomo et al. 2016). The developed ADL-CNN model is rarer than traditional state-of-art CNN models. It has been shown that significantly higher ACC results are achieved when comparing the state-of-the-art systems in identifying the relevant lesions of DR and classifying the severity-level of DR. The ADL-CNN model correctly determined almost all of the test images for the five-stages DR severity-level classifications and reached an effective SE and SP for individual evaluation.

According to the results given in Table 5 of the proposed ADL-CNN system eliminated the necessity of human classifier in image analysis and produced clinically acceptable results with 99.66% ACC, 93.76% SE, and 96.71% SP values. Thus, the risk of misinterpretation of retinal samples during the diagnosis of patients with DR can be reduced and the initiation of treatment can be accelerated. If we emphasize the strengths of the proposed method in this study, the most important feature is that it converges with the model much earlier than state-of-art methods. Moreover, reaching the best local optimum value with the SGD scheme used to select the most informative patches at a high level is the biggest advantage of basic training. Another important advantage of the model is the use of viable masks for the prediction of segmented DR lesions. As given in Tables 2 and 7, the third major advan-

tage of ADL-CNN is that achieves higher accuracy compared to existing pre-trained CNN models that perform five different levels of DR classification. However, when the results in Table 2 are examined, the SE (93) result obtained from our proposed method was lower than the existing robust studies, especially in the moderate, severe, and PDR classes, due to the weak separation between the overlapping regions of HEMs and MAs (Li et al. 2019a, b; Gulshan et al. 2016).

It can be easily said that DL methods that adopt an end-to-end training approach produce relatively lower ACC, SE, and SP results with the findings obtained as a result of detailed research (Akilesh et al. 2017; Orlando et al. 2018; Wang et al. 2017). In this case, the failure of the network model to learn retinal features in the eye vascular systems results in the inability to localize the ROIs, resulting in the failure of DR lesion detection and segmentation. TL was used in the beginning, especially in the tasks of recognizing various objects in nature, such as living things and plants. Experimental results obtained in studies have revealed that TL is not sufficient for the classification of real-time medical images. Results from these studies using TL techniques could not represent a valid system for the classification of the five severity levels of DR (Gulshan et al. 2016; He et al. 2016; Hu et al. 2018; Huang et al. 2017).

The ADL-CNN method can produce high results in terms of computational costs in the case of processing large-scale data. However, this disadvantage can be avoided by using only certain samples of the data through standard sampling methods. It is thought that the application of this data selection method with TL will increase the learning performance. It was observed that the ADL-CNN system failed to classify some images, especially at moderate, severe, and PDR DR severity levels. The main reason for this is that although preprocessing has been applied to the images, especially these images have low contrast and contain complex patterns. It is planned to use perceptually oriented color space to produce higher RGB color content from images belonging to these classes in future studies to solve this problem. Moreover, the Transformers method can also be used instead of CNN which allows the processing of multiple modalities (for example, images, videos, text, and speech) using similar processing blocks with its simple design.

6 Conclusions

Determining the DR intensity level from color fundoscopic images is an important consideration in this field. However, the presence of complex lesion structures in color images on fundus imaging makes it difficult to detect the five severity levels of DR. Most existing studies in the literature consider only two classes for DR classification. In this study, the ABC algorithm, which calculates a threshold value according to the results of some image preprocessing and image histograms, was applied to improve the quality of color fundus images and reveal the defining lesion features of DR before ADL. Then, using this threshold value, segmented images of DR-determining lesion features were obtained. Proposed ADL-CNN simultaneously and automatically detects the five severity levels of DR, which has a 7-layer CNN architecture in which the dataset is used with the localization of lesions by selecting some basic annotated fundoscopic samples instead of all the training samples. In this method, the locations of the lesions and the DR were determined using fundus samples with some ground-truth annotated. Initially, entrance fundus images were subjected to

various preprocessing to increase uniform color contrast. Then, these preprocessed images fed the model to learn the distinguishing features. The performance of the proposed ADL-CNN method was tested on the EyePACS dataset consisting of 35,122 images. As given in Chap. 4, the experimental results were evaluated in terms of ACC, SE, SP, and F-measure, and quite good performance was obtained. The proposed ADL-CNN method can be developed in the future for DR detection with different CNN settings and can be used in different multimedia applications.

Declarations

Conflict of interest The authors declare there is no conflicts of interest.

References

Abbas Q, Fondon I, Sarmiento A, Jiménez S, Alemany P (2017) Automatic recognition of severity level for diagnosis of diabetic retinopathy using deep visual features. Med Biol Eng Comput Nov 55(11):1959–1974

Akilesh B, Marwah T, Balasubramanian VN, Rajamani K (2017) On the relevance of very deep networks for diabetic retinopathy diagnostics. Applications of Cognitive Computing Systems and IBM Watson. Springer, Singapore, pp 47–54

Alyoubi WL, Abulkhair MF, Shalash WM (2021) Diabetic Retinopathy Fundus Image Classification and Lesions Localization System. Using Deep Learning Sensors 21(11):3704

Alyoubi WL, Shalash WM, Abulkhair MF (2020) Diabetic retinopathy detection through deep learning techniques: A review Informatics in Medicine Unlocked, 20, 100377

Annapoorani MC, Bobby JS, Anandhi B, Hema P (2021) Deep Multiple Instance Learning for Automatic Detection of Diabetic Retinopathy in Retinal Images Annals of the Romanian Society for Cell Biology. 25:13696–137096

Bakator M, Radosav D (2018) Deep learning and medical diagnosis: A review of literature Multimodal Technologies and Interaction, 2(3), 47

Bello-Cerezo R, Bianconi F, Di Maria F, Napoletano P, Smeraldi F (2019) Comparative evaluation of hand-crafted image descriptors vs off-the-shelf CNN-based features for colour texture classification under ideal and realistic conditions. Appl Sci 9(4):738

Bhaskaranand M, Ramachandra C, Bhat S, Cuadros J, Nittala MG, Sadda S, Solanki K (2016) Automated diabetic retinopathy screening and monitoring using retinal fundus image analysis. J Diabetes Sci Technol 10(2):254–261

Blair M (2016) Diabetes mellitus review Urologic nursing, 36(1)

Bodapati JD, Shaik NS, Naralasetti V (2021) Composite deep neural network with gated-attention mechanism for diabetic retinopathy severity classificationJournal of Ambient Intelligence and Humanized Computing,1–15

Cao W, Czarnek N, Shan J, Li L (2018) Microaneurysm detection using principal component analysis and machine learning methods. IEEE Trans Nanobiosci 17(3):191–198

Cengil E, Çınar A, Özbay E (2017) October) Image classification with caffe deep learning framework In 2017 International Conference on Computer Science and Engineering (UBMK) (pp 440–444) IEEE

Chandrakumar T, Kathirvel RJIJERT (2016) Classifying diabetic retinopathy using deep learning architecture. Int J Eng Res Technol 5(6):19–24

Christine N (2015) Access our diverse and vast retinal image database for your research needs https://www.eyepacscom/data-analysis Accessed 26 Oct 2021

Cockburn D (2013) Handbook of Retinal Screening in Diabetes: Diagnosis and Management, by Roy Taylor and Deborah Batey Hoboken, New Jersey: Wiley-Blackwell, 2012 173 pages, 9995

Cole JB, Florez JC (2020) Genetics of diabetes mellitus and diabetes complications. Nat Rev Nephrol 16(7):377–390

Congdon NG, Friedman DS, Lietman T (2003) Important Causes of Visual Impairment in the World Today JAMA. JAMA 290(15):2057–2060

Das S, Kharbanda K, Suchetha M, Raman R, Dhas E (2021) Deep learning architecture based on segmented fundus image features for classification of diabetic retinopathy. Biomed Signal Process Control 68:102600

Decenciere E, Cazuguel G, Zhang X, Thibault G, Klein JC, Meyer F, Chabouis A (2013) TeleOphta: Machine learning and image processing methods for teleophthalmology Irbm, 34(2), 196–203

Dekhil O, Naglah A, Shaban M, Ghazal M, Taher F, Elbaz A (2019) December) Deep learning based method for computer aided diagnosis of diabetic retinopathy In 2019 IEEE International Conference on Imaging Systems and Techniques (IST) (pp 1–4) IEEE

Deng J, Dong W, Socher R, Li LJ, Li K, Fei-Fei L (2009) June) Imagenet: A large-scale hierarchical image database In 2009 IEEE conference on computer vision and pattern recognition (pp 248–255) Ieee

Deng L, Yu D (2014) Deep learning: methods and applications Foundations and trends in signal processing, 7(3–4), 197–387

Freytak A, Rodner E, Denzler J (2014) September) Selecting influential examples: Active learning with expected model output changes In European conference on computer vision (pp 562–577) Springer, Cham

Galveia JN, Travassos A, Quadros FA, da Silva Cruz LA (2018) Computer aided diagnosis in ophthalmology: Deep learning applications. Classification in BioApps. Springer, Cham, pp 263–293

Goatman KA, Fleming AD, Philip S, Williams GJ, Olson JA, Sharp PF (2010) Detection of new vessels on the optic disc using retinal photographs. IEEE Trans Med Imaging 30(4):972–979

Greenspan H, Van Ginneken B, Summers RM (2016) Guest editorial deep learning in medical imaging: Overview and future promise of an exciting new technique. IEEE Trans Med Imaging 35(5):1153–1159

Gulshan V, Peng L, Coram M, Stumpe MC, Wu D, Narayanaswamy A, Webster DR (2016) Development and validation of a deep learning algorithm for detection of diabetic retinopathy in retinal fundus photographs Jama. 316:2402–241022

Guo S, Li T, Kang H, Li N, Zhang Y, Wang K (2019) L-Seg: An end-to-end unified framework for multi-lesion segmentation of fundus images Neurocomputing. 349:52–63

Haneda S, Yamashita H (2010) International clinical diabetic retinopathy disease severity scale Nihon. rinsho Japanese journal of clinical medicine 68:228–235

Harangi B, Toth J, Baran A, Hajdu A (2019) July) Automatic screening of fundus images using a combination of convolutional neural network and hand-crafted features In 2019 41st Annual International Conference of the IEEE Engineering in Medicine and Biology Society (EMBC) (pp 2699–2702) IEEE

He A, Li T, Li N, Wang K, Fu H (2020) CABNet: Category attention block for imbalanced diabetic retinopathy grading. IEEE Trans Med Imaging 40(1):143–153

He K, Zhang X, Ren S, Sun J (2015) Delving deep into rectifiers: Surpassing human-level performance on imagenet classification In Proceedings of the IEEE international conference on computer vision (pp 1026–1034)

He K, Zhang X, Ren S, Sun J (2016) Deep residual learning for image recognition In Proceedings of the IEEE conference on computer vision and pattern recognition (pp 770–778)

Hsieh YT, Chuang LM, Jiang YD, Chang TJ, Yang CM, Yang CH, Chen M (2021) Application of deep learning image assessment software VeriSee™ for diabetic retinopathy screening. J Formos Med Assoc 120(1):165–171

Hu J, Shen L, Sun G (2018) Squeeze-and-excitation networks In Proceedings of the IEEE conference on computer vision and pattern recognition (pp 7132–7141)

Huang G, Liu Z, Van Der Maaten L, Weinberger KQ (2017) Densely connected convolutional networks In Proceedings of the IEEE conference on computer vision and pattern recognition (pp 4700–4708)

Jiang H, Yang K, Gao M, Zhang D, Ma H, Qian W (2019) July) An interpretable ensemble deep learning model for diabetic retinopathy disease classification In 2019 41st Annual International Conference of the IEEE Engineering in Medicine and Biology Society (EMBC) (pp 2045–2048) IEEE

Kar SS, Maity SP (2018) Gradation of diabetic retinopathy on reconstructed image using compressed sensing. IET Image Proc 12(11):1956–1963

Karaboga D (2010) Artificial bee colony algorithm scholarpedia, 5(3), 6915

Kassani SH, Kassani PH, Khazaeinezhad R, Wesolowski MJ, Schneider KA, Deters R (2019) December) Diabetic retinopathy classification using a modified xception architecture In 2019 IEEE International Symposium on Signal Processing and Information Technology (ISSPIT) (pp 1–6)

Kermany DS, Goldbaum M, Cai W, Valentim CC, Liang H, Baxter SL, Zhang K (2018) Identifying medical diagnoses and treatable diseases by image-based deep learning Cell, 172(5), 1122–1131

Khan SH, Abbas Z, Rizvi SD (2019) February) Classification of diabetic retinopathy images based on customised CNN architecture In 2019 Amity International Conference on Artificial Intelligence (AICAI) (pp 244–248) IEEE

Khomri B, Christodoulidis A, Djerou L, Babahenini MC, Cheriet F (2018) Retinal blood vessel segmentation using the elite-guided multi-objective artificial bee colony algorithm. IET Image Proc 12(12):2163–2171

Krizhevsky A, Sutskever I, Hinton GE (2017) ImageNet classification with deep convolutional neural networks. Commun ACM 60(6):84–90
Li B, Li HK (2013) Automated analysis of diabetic retinopathy images: principles, recent developments, and emerging trends Current diabetes reports. 13:453–4594
Li T, Bo W, Hu C, Kang H, Liu H, Wang K, Fu H (2021) Applications of deep learning in fundus images. A review Medical Image Analysis, p 101971
Li T, Gao Y, Wang K, Guo S, Liu H, Kang H (2019a) Diagnostic assessment of deep learning algorithms for diabetic retinopathy screening Information Sciences. 501:511–522
Li X, Hu X, Yu L, Zhu L, Fu CW, Heng PA (2019b) CANet: cross-disease attention network for joint diabetic retinopathy and diabetic macular edema grading IEEE transactions on medical imaging. 39:1483–14935
Li Z, Keel S, Liu C, He Y, Meng W, Scheetz J, He M (2018) An automated grading system for detection of vision-threatening referable diabetic retinopathy on the basis of color fundus photographs Diabetes care, 41(12), 2509–2516
Lin CH, Mausam M, Weld DS (2016) February) Re-active learning: Active learning with relabeling In Thirtieth AAAI Conference on Artificial Intelligence
Lin J, Yu L, Weng Q, Zheng X (2020) Retinal image quality assessment for diabetic retinopathy screening: A survey Multimedia. Tools and Applications 79(23):16173–16199
Litjens G, Kooi T, Bejnordi BE, Setio AAA, Ciompi F, Ghafoorian M, Sánchez CI (2017) A survey on deep learning in medical image analysis Medical image analysis, 42, 60–88
Liu YP, Li Z, Xu C, Li J, Liang R (2019) Referable diabetic retinopathy identification from eye fundus images with weighted path for convolutional neural network Artificial intelligence in medicine, 99, 101694
Lu L, Zheng Y, Carneiro G, Yang L (2017) Deep learning and convolutional neural networks for medical image computing Advances in computer vision and pattern recognition. 10:978–973
Majumder S, Kehtarnavaz N (2021) Multitasking Deep Learning Model for Detection of Five Stages of Diabetic Retinopathy arXiv preprint arXiv:210304207
Mansour RF (2018) Deep-learning-based automatic computer-aided diagnosis system for diabetic retinopathy. Biomed Eng Lett 8(1):41–57
Mateen M, Wen J, Hassan M, Nasrullah N, Sun S, Hayat S (2020) Automatic detection of diabetic retinopathy: a review on datasets, methods and evaluation metrics. IEEE Access 8:48784–48811
Mookiah MRK, Acharya UR, Chua CK, Lim CM, Ng EYK, Laude A (2013) Computer-aided diagnosis of diabetic retinopathy: A review Computers in biology and medicine. 43:2136–215512
Orlando JI, Prokofyeva E, Del Fresno M, Blaschko MB (2018) An ensemble deep learning based approach for red lesion detection in fundus images Computer methods and programs in biomedicine. 153:115–127
Otálora S, Perdomo O, González F, Müller H (2017) Training deep convolutional neural networks with active learning for exudate classification in eye fundus images. Intravascular Imaging and Computer Assisted Stenting, and Large-Scale Annotation of Biomedical Data and Expert Label Synthesis. Springer, Cham, pp 146–154
Otsu N (1979) A threshold selection method from gray-level histograms. IEEE Trans Syst man cybernetics 9(1):62–66
Perdomo O, Otalora S, Rodríguez F, Arevalo J, González FA (2016) A novel machine learning model based on exudate localization to detect diabetic macular edema
Pires R, Avila S, Wainer J, Valle E, Abramoff MD, Rocha A (2019) A data-driven approach to referable diabetic retinopathy detection Artificial intelligence in medicine. 96:93–106
Pires R, Jelinek HF, Wainer J, Goldenstein S, Valle E, Rocha A (2013) Assessing the need for referral in automatic diabetic retinopathy detection. IEEE Trans Biomed Eng 60(12):3391–3398
Porwal P, Pachade S, Kokare M, Deshmukh G, Son J, Bae W, Meriaudeau F (2020) Idrid: Diabetic retinopathy–segmentation and grading challenge Medical image analysis, 59, 101561
Pratt H, Coenen F, Broadbent DM, Harding SP, Zheng Y (2016) Convolutional neural networks for diabetic retinopathy Procedia computer science. 90:200–205
Raju M, Pagidimarri V, Barreto R, Kadam A, Kasivajjala V, Aswath A (2017) Development of a deep learning algorithm for automatic diagnosis of diabetic retinopathy In MEDINFO 2017: Precision Healthcare through Informatics. IOS Press, pp 559–563
Sánchez CI, Niemeijer M, Abràmoff MD, van Ginneken B (2010 September) Active learning for an efficient training strategy of computer-aided diagnosis systems: application to diabetic retinopathy screening In International Conference on Medical Image Computing and Computer-Assisted Intervention (pp 603–610) Springer, Berlin, Heidelberg
Sankar M, Batri K, Parvathi R (2016) Earliest diabetic retinopathy classification using deep convolution neural networks pdf. Int J Adv Eng Technol 10:M9
Settles B, Craven M, Ray S (2007) Multiple-instance active learning Advances in neural information processing systems. 20:1289–1296

Shanthi T, Sabeenian RS (2019) Modified Alexnet architecture for classification of diabetic retinopathy images. Comput Electr Eng 76:56–64
Sikder N, Masud M, Bairagi AK, Arif ASM, Nahid AA, Alhumyani HA (2021) Severity Classification of Diabetic Retinopathy Using an Ensemble Learning Algorithm through. Analyzing Retinal Images Symmetry 13(4):670
Sinclair A, Saeedi P, Kaundal A, Karuranga S, Malanda B, Williams R (2020) Diabetes and global ageing among 65–99-year-old adults: Findings. 162:108078from the International Diabetes Federation Diabetes Atlas Diabetes research and clinical practice
Singh N, Kaur L, Singh K (2019) Histogram equalization techniques for enhancement of low radiance retinal images for early detection of diabetic retinopathy Engineering Science and Technology. Int J 22(3):736–745
Snow E, Alam M, Glandon A, Iftekharuddin K (2020) July) End-to-end Multimodel Deep Learning for Malware Classification In 2020 International Joint Conference on Neural Networks (IJCNN) (pp 1–7) IEEE
Sreelatha P, Bhuvaneswari P, Venugopal E, Pattanaik B, Kumar TP (2021) Diabetic Retinopathy Detection: Solutions Through Application of Meta-Heuristic Approaches Annals. of the Romanian Society for Cell Biology, pp 4353–4361
Sundar KS, Bonta LR, Baruah PK, Sankara SS (2018) March) Evaluating training time of Inception-v3 and Resnet-50,101 models using TensorFlow across CPU and GPU In 2018 Second International Conference on Electronics, Communication and Aerospace Technology (ICECA) (pp 1964–1968) IEEE
Ting DSW, Cheung GCM, Wong TY (2016) Diabetic retinopathy: global prevalence, major risk factors, screening practices and public health challenges: a review. Clin Exp Ophthalmol 44(4):260–277
TSai PW, Pan JS, Liao BY, Chu SC (2009) Enhanced artificial bee colony optimization. Int J Innovative Comput Inform Control 5(12):5081–5092
Vaishnavi J, Subban R, Anousouya M, Stephen P (2016) Automatic Assessment of Non-proliferative Diabetic Retinopathy using Modified ABC Algorithm with Feed Forward Neural Network International Conference on Advances in Computational Intelligence and Communication 16–21
Vega R, Sanchez-Ante G, Falcon-Morales LE, Sossa H, Guevara E (2015) Retinal vessel extraction using lattice neural networks with dendritic processing Computers in biology and medicine. 58:20–30
Wan S, Liang Y, Zhang Y (2018) Deep convolutional neural networks for diabetic retinopathy detection by image classification. Comput Electr Eng 72:274–282
Wang J, Luo J, Liu B, Feng R, Lu L, Zou H (2020) Automated diabetic retinopathy grading and lesion detection based on the modified R-FCN object-detection algorithm IET Computer Vision. 14:1–81
Wang X, Lu Y, Wang Y, Chen WB (2018) July) Diabetic retinopathy stage classification using convolutional neural networks In 2018 IEEE International Conference on Information Reuse and Integration (IRI) (pp 465–471) IEEE
Wang Z, Yin Y, Shi J, Fang W, Li H, Wang X (2017) September) Zoom-in-net: Deep mining lesions for diabetic retinopathy detection In International Conference on Medical Image Computing and Computer-Assisted Intervention (pp 267–275) Springer, Cham
Washington RE, Orchard TJ, Arena VC, LaPorte RE, Secrest AM, Tull ES (2014) All-cause mortality in a population-based type 1 diabetes cohort in the US Virgin Islands Diabetes research and clinical practice. 103:504–5093
Wisaeng K, Sa-Ngiamvibool W (2019) Exudates detection using morphology mean shift algorithm in retinal images. IEEE Access 7:11946–11958
Xiao Z, Xu X, Zhang H, Szczerbicki E (2021) A new multi-process collaborative architecture for time series classification. Knowl Based Syst 220:106934
Yu F, Seff A, Zhang Y, Song S, Funkhouser T, Xiao J (2015) Lsun: Construction of a large-scale image dataset using deep learning with humans in the loop arXiv preprint arXiv:150603365
Zago GT, Andreão RV, Dorizzi B, Salles EOT (2020) Diabetic retinopathy detection using red lesion localization and convolutional neural networks Computers in biology and medicine, 116, 103537
Zhang H, Xiao Z, Wang J, Li F, Szczerbicki E (2019a) A novel IoT-perceptive human activity recognition (HAR) approach using multihead convolutional attention. IEEE Internet of Things Journal 7(2):1072–1080
Zhang Q (2018) January) Convolutional neural networks In Proceedings of the 3rd International Conference on Electromechanical Control Technology and Transportation (pp 434–439)
Zhang W, Zhong J, Yang S, Gao Z, Hu J, Chen Y, Yi Z (2019b) Automated identification and grading system of diabetic retinopathy using deep neural networks. Knowl Based Syst 175:12–25
Zhou S, Chen Q, Wang X (2014) Active semi-supervised learning method with hybrid deep belief networksPloS one, 9(9), e107122